

# Phase estimation for a phased array therapeutic interstitial ultrasound probe

Zhenya Yang and Jean-Louis Dillenseger

**Abstract**—This paper deals about high intensity ultrasound interstitial therapy simulation. The simulated phased array ultrasound probe allows a dynamic electronic focusing of the therapeutic beam. In order to maximize the power deposit at the focal point we propose a method which allows to optimally defining the phase shift of the electrical control signal for each individual element.

## I. INTRODUCTION

The hepatocellular carcinoma (HCC) is a liver parenchyma cell tumor. This tumor can curatively treated by a partial liver ablation [1]. When the tumor is confined to a solitary mass, it can be potentially curable by a percutaneous surgical resection. Ultrasound therapy is now proposed within this interstitial applicators context [2]. This therapy allows a better control in power and direction than the other interstitial techniques (radio frequency and so on). The first interstitial ultrasonic probes were mono-element but new generations of phased array probes have now being developed. The increasing of the probe elements number (5 or more) allows enhancing the capacity of the beam deflection and therefore a better control of the therapy [3].

Like any minimally invasive surgery, an interstitial ultrasonic ablation will need the definition of a precise preoperative planning. This preoperative planning can be established using a simulation tool that allows, if it is realistic enough, to design and try different therapy strategies and so to define the future parameters of the procedure. In a preliminary study, the simulation of the effect of a 64 elements probe has been proposed (Fig. 1-left) [4]. In this study, the beam deflection was classically obtained by a specific delay time (a phase shift) for firing each group of elements in order to synchronize the various ultrasound waves at a focal point chosen by the user. But the phase rule used to define the specific phase shifts was not optimal in the sense of the presence of many side lobes. In this paper, we propose a new method to better estimate the phase shifts and thus to optimize the energy deposit.

## II. MATERIALS AND METHODS

The simulation of the effects of a therapeutic ultrasound therapy is usually based on [5]: 1) the simulation of the pressure field generated by the transducer, 2) the estimation of the temperature evolution over time (by solving Pennes' bioheat transfer equation -BHTE) and 3) the estimation of the induced necrosis. If the heat equation solving and the

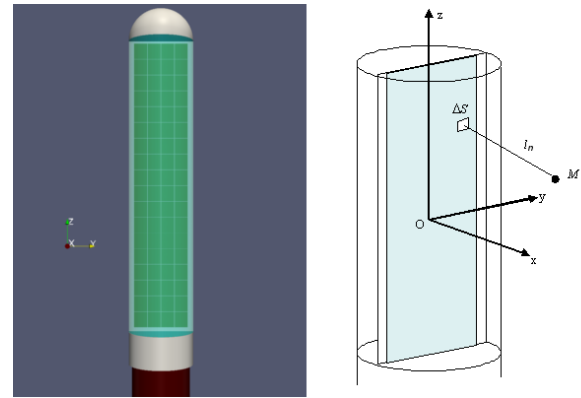


Fig. 1. 3D view of the 64 elements ultrasound therapy probe (left) [4]. Ultrasound probe geometry and coordinate system (right).

necrosis estimation are standard calculations in hyperthermia, the simulation of the acoustic pressure field is specific to the ultrasound therapies.

### A. Acoustic pressure field estimation

A simulated phased array transducer will have  $N$  elements  $E_i$  ( $1 \leq i \leq N$ ). Each element is driven by a generator which produces a pressure wave with an amplitude  $p_i$  and a phase shift  $\varphi_i$ . The consequence of this command phase shift  $\varphi_i$  is a spatial shift of the ultrasound wave by a value of  $\frac{\varphi_i}{2\pi} \lambda$  ( $\lambda$  the wavelength). A dynamic focusing can be obtained by setting a phase shift specific to each element  $E_i$  (the phase law).

The goal is thus to compute the acoustic pressure at a location point  $M$  (Fig. 1-right). Because of the relatively low power of the input transducer pressure and the non-focusing geometry of the probe, the propagation can be considered linear and the pressure field can be exactly computed on the basis of the Rayleigh integral [5]. Each element  $E_i$  of the transducer is sampled into  $N_i$  elementary surfaces elements  $S_n$  which size  $\Delta S$  is negligible in comparison with the wavelength  $\lambda$ . Each  $S_n$  can so be considered as a single emitter with a pressure at the transducer surface  $p_i$  (in Pa) and a phase shift  $\varphi_i$  (in this case  $S_n$  is a sample of element  $E_i$ ).  $S_n$  is connected to  $M$  by a straight segment of length  $l_n$ . For simplicity and for reducing the computational time, we will assume that the tissues are homogeneous (the ultrasound propagation speed and so the wavelength  $\lambda$  and the tissue ultrasound attenuation coefficient  $\alpha$  are considered constant). The acoustic pressure at the point  $M$  can be exactly computed by:

Z. Yang and J.-L. Dillenseger are with INSERM, U1099, Rennes, F-35000, France and Université de Rennes 1, LTSI, Rennes, F-35000, France. jean-louis.dillenseger@univ-rennes1.fr

$$p(M) = \left| \sum_{i=1}^N \sum_{n=1}^{N_i} j \frac{p_i}{\lambda} \Delta S \frac{\exp^{-j(kl_n + \varphi_i)}}{l_n} \exp^{-f\alpha l_n} \right| \quad (1)$$

where:  $\lambda$  is the wavelength (m),  $f$  the frequency (Hz),  $k$  the wave number ( $2\pi/\lambda$ ) and  $\alpha$  the tissue attenuation coefficient in ( $\text{Np} \cdot \text{cm}^{-1} \cdot \text{MHz}^{-1}$ ). Two terms can be seen in (1). The expression  $\exp^{-j(kl_n + \varphi_i)}/l_n$  is the phase term which will be important for the focusing. The second expression,  $\exp^{-f\alpha l_n}$ , simulates the ultrasound attenuation by the tissue.

### B. Phase shift estimation

The focusing on a point  $F$  is to maximize the acoustic power on that point.

The obvious idea is to consider that the ultrasound wave is emitted from the center  $O_i$  of each probe element  $E_i$ . Each wave is phase shifted in order to synchronize all the waves on  $F$ . For this, and for each  $E_i$ , the Euclidean distance  $\|O_i F\|$  between  $O_i$  and  $F$  is computed. The phase shift is then estimated by:

$$\varphi_i = 2\pi(\|O_i F\| \% \lambda) \quad (2)$$

where  $\%$  is the modulo operation (the remainder of the division).

However, we found by simulation that the pressure is usually not maximum at the focal point when we use the phase shift estimation method described in (2). This phenomenon can be explained by the fact that an element  $E_i$  cannot be reduced to its center. The element size is very large compared to  $\lambda$ . Each element generates so its own interference. To ensure a maximum pressure at the focal point, the element size and shape must be taken into account when estimating the phase shift.

Using (1) to calculate the pressure at the focal point  $F$  and applying the Euler transformation, we obtain:

$$p(F) = \left| \sum_{i=1}^N j p r_i(F) - p i_i(F) \right| \quad (3)$$

with  $p r_i(F)$  and  $p i_i(F)$  respectively the real and imaginary parts of the pressure generated by an element  $E_i$ :

$$p r_i(F) = \sum_{n=1}^{N_i} \frac{p_i \Delta S \exp^{-f\alpha l_n}}{\lambda l_n} \cos(kl_n + \varphi_i)$$

$$p i_i(F) = \sum_{n=1}^{N_i} \frac{p_i \Delta S \exp^{-f\alpha l_n}}{\lambda l_n} \sin(kl_n + \varphi_i)$$

Using the angle transformation formula,  $p r_i(F)$  can be rewritten as:

$$p r_i(F) = \sum_{n=1}^{N_i} b_n \cos(kl_n) \cos(\varphi_i) - b_n \sin(kl_n) \sin(\varphi_i)$$

with

$$b_n = \frac{p_i \Delta S \exp^{-f\alpha l_n}}{\lambda l_n}$$

and then as:

$$p r_i(F) = \sqrt{c_i^2 + d_i^2} \cos\left(\varphi_i + \arctan\left(\frac{c_i}{d_i}\right)\right) \quad (4)$$

with

$$c_i = \sum_{n=1}^{N_i} \frac{p_i \Delta S \exp^{-f\alpha l_n}}{\lambda l_n} \sin(kl_n) \quad (5)$$

$$d_i = \sum_{n=1}^{N_i} \frac{p_i \Delta S \exp^{-f\alpha l_n}}{\lambda l_n} \cos(kl_n) \quad (6)$$

In the same way:

$$p i_i(F) = -j \sqrt{c_i^2 + d_i^2} \cos\left(\varphi_i - \arctan\left(\frac{d_i}{c_i}\right)\right) \quad (7)$$

If we consider (3), (4) and (7), the synchronization at the focal point  $F$  of all the elements  $E_i$  (and therefore the optimum phase shifts) can be obtained by imposing for example all the imaginary parts  $p i_i(F)$  equal to zero:

$$\varphi_{opti_i} = \frac{\pi}{2} + \arctan\left(\frac{d_i}{c_i}\right) \quad (8)$$

## III. RESULTS - DISCUSSION

We simulate the pressure field induced by a 64-elements  $3\text{mm} \times 18\text{mm}$  interstitial probe. The elements have a central frequency of 5MHz and deliver a pressure at the transducer surface  $p_i = 20\text{W} \cdot \text{cm}^{-2}$  [3]. The elements are spatially distributed as an array of 4 columns and 16 lines (Fig. 1-left). The virtual probe is centered in a  $80\text{mm} \times 80\text{mm} \times 24\text{mm}$  volume which is regularly sampled with a 0.4mm sampling step on  $201 \times 201 \times 61$  points. For each simulation, the phase shifts are adjusted to focus the beam onto a one 3D point within that volume.

The evaluation protocol is as following: we compute the acoustic pressure at several focal points within the volume. On these points we compare the acoustic pressure obtained with our optimized phase shifts estimation method (8) (we will call it *Optimized phase* in the rest of the paper) with the naive method (2) (*Classical phase* in the rest of the paper)). The results can be seen on Table I. Our method gives better results than the classical phase shift estimation especially for focal points located less than 30mm from the probe. In fact, for focal points close to the probe surface, we are in a near field case and therefore the waves originating from the same single element face generate their own interference. Taking the element size into account for the phase shifts estimation allows optimizing the interferences at the focal point.

Fig. 2 and Fig. 3 show the dynamic focusing ability of our 64-elements probe model. The various sub-figures represent on the  $x - z$  transverse sections with  $y = 0$  (see the coordinate system on Fig. 1), respectively, the pressure map (color scale black-blue-red-yellow-white from 0 to 2, 500kPa) and the temperature map (color scale black-blue-red-yellow-white from 37°C to 100°C) after firing 20s. Two cases are presented with two different focus points

TABLE I

COMPARISON BETWEEN THE PRESSURES COMPUTED AT THE FOCAL POINT OBTAINED USING THE CLASSICAL AND OPTIMIZED PHASE SHIFTS ESTIMATION.

Focal point coordinate ( $x, y, z$ in mm)	Classical phase ( $10^6$ Pa)	Optimized phase ( $10^6$ Pa)
(5, 0, 0)	1.15	2.53
(10, 0, 0)	1.43	2.23
(15, 0, 0)	1.12	1.94
(20, 0, 0)	1.17	1.65
(30, 0, 0)	1.20	1.20

highlighted in black in the temperature maps:  $F_1 = (15\text{mm}, 0\text{mm}, 0\text{mm})$  which is on the central axis (Fig. 2) and  $F_2 = (15\text{mm}, 0\text{mm}, -4\text{mm})$  where the beam is deflected on the  $z$  axis (Fig. 3). The top rows of both figures show the results when the phase shifts are estimated using the classical method. On the bottom rows the phase shifts are estimated using our proposed method.

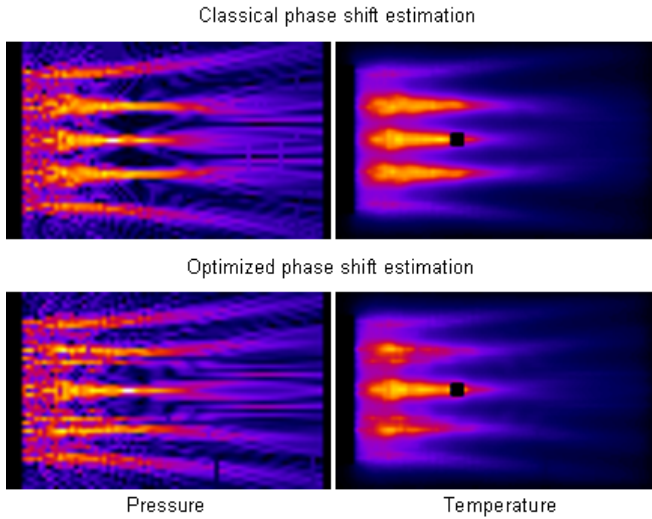


Fig. 2. Pressure map and temperature map within the  $x - z$  transverse plane when shooting on the (15mm, 0mm, 0mm) focus points. The focus point is the black dot in the temperature maps. On top with the classical phase shift estimation method, on bottom with the optimized one. The color scale black-blue-red-yellow-white corresponds from 0 to 2,500kPa for the pressure map and from  $37^\circ\text{C}$  to  $100^\circ\text{C}$  for the temperature map.

The number of elements in the  $z$  direction (16 lines) is not sufficient to ensure a good focus without side lobes. The side lobes are caused by interferences between the signals emitted by the several elements. On Fig. 2, they are 2 couples of pressure side lobes over and under the main lobe. These lobes produce two supplementary temperature hot spots on either side of the focus point. However, it can be clearly seen that our optimal method allows to increase the energy deposit at the focal point and to reduce the size of the side lobes.

The presence of side lobes is even more pronounced when the focal point is deflected on the  $z$  direction. On Fig. 3, it can be seen that the classical method induces two side lobes above the focal point. These two side lobes have a

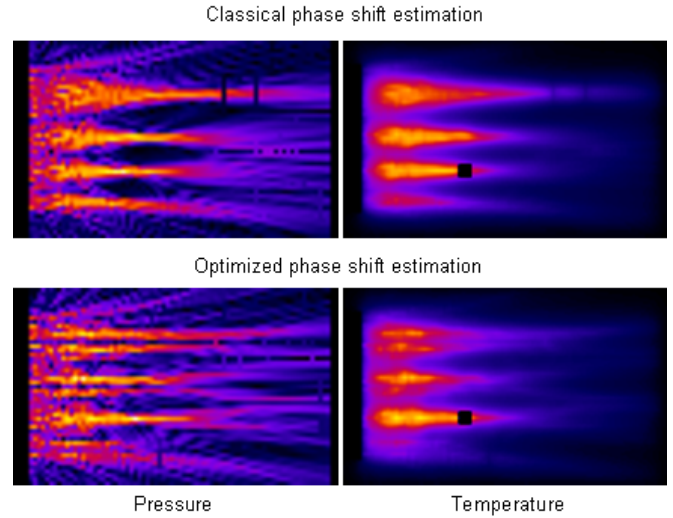


Fig. 3. Pressure map and temperature map within the  $x - z$  transverse plane when shooting on the (15mm, 0mm, -4mm) focus points. The focus point is the black dot in the temperature maps. On top with the classical phase shift estimation method, on bottom with the optimized one. The color scales are the same as previously.

size bigger than the main lobe, so the temperature hot spots. With the optimized method, these two side lobes are really smaller because it better controls the interferences between the elements.

We made also a simulation with a spatial distribution of the elements as an array of 1 column and 64 lines. This distribution is more optimal for focusing along the  $z$  direction because they are more element in that direction and also because the element size is smaller in that direction. Fig. 4 shows the  $x - z$  transverse section of the pressure maps when the power deposit is focused on  $F_2 = (15\text{mm}, 0\text{mm}, -4\text{mm})$  (the same focus point as in Fig. 3). With a higher number of elements in the  $z$  direction, it can be seen that only a side lobe remains (on the top of the transverse section). This side lobe is relatively diffuse and far from the focal point. In this simulation, the pressure maps obtained using both phase shifts estimation methods are very similar with a maximum at the focal point of 5,180kPa and 5,210kPa respectively for the classical and optimized method. In the maps the pressure levels higher than 2,500kPa have been cropped to keep the

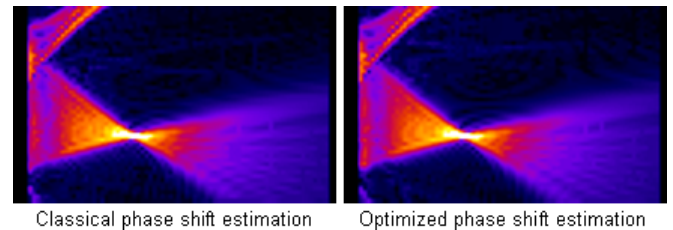


Fig. 4. Pressure maps within the  $x - z$  transverse plane when shooting with an array of  $1 \times 64$  elements on the (15mm, 0mm, -4mm) focus point. On the right with the classical phase shift estimation method, on the left with the optimized one. The color scales are the same as previously but the pressure levels higher than 2,500kPa have been cropped.

same color scale as previously. We can see that when the elements size is small we are no more in a near field case and the self-interferences induced by a single element decrease and so the need of an optimal phase shifts estimation seems to be less useful.

The results presented here are theoretical and validated only on simulations. Further studies should be performed on a real device and in a real situation. However it is well known by the people dealing with multi-elements therapeutic ultrasound devices that the classical obvious phase shift estimation method is not optimal. Usually they tune manually the phase shifts with help of a hydrophone. We propose a direct phase shifts estimation based on simulation. For a more precise usage, it can be seen on (5) and (6) that tissues inhomogeneities (different ultrasound attenuation coefficients  $\alpha$ ) could be integrated within the optimized phase shifts estimation.

#### IV. CONCLUSIONS

We proposed a new approach for determining the optimal phase shifts used to drive the focusing of an ultrasonic phased array probe. The simulations showed that when the phase shifts are estimated with our method, more energy can be

deposited at the focal point and the side lobes size are decreased.

#### ACKNOWLEDGMENT

This work is part of the French MULTIP project supported by an ANR Grant (ANR-09-TECS-011).

#### REFERENCES

- [1] E. Mor, R. T. Kasper, P. Sheiner, and M. Schwartz, "Treatment of hepatocellular carcinoma associated with cirrhosis in the era of liver transplantation," *Annals of Internal Medicine*, vol. 129, no. 8, pp. 643–653, 1998.
- [2] C. Lafon, J. Y. Chapelon, F. Prat, F. Gorry, Y. Theillere, and D. Cathignol, "Design and in vitro results of a high intensity ultrasound interstitial applicator," *Ultrasonics*, vol. 36, no. 1-5, pp. 683–687, 1998.
- [3] NR Owen, JY Chapelon, G. Bouchoux, R. Berriet, G. Fleury, and C. Lafon, "Dual-mode transducers for ultrasound imaging and thermal therapy," *Ultrasonics*, vol. 50, no. 2, pp. 1–5, 2010.
- [4] S. Esneault, C. Lafon, and J.-L. Dillenseger, "Modélisation spécifique patient des effets d'une thérapie interstitielle par une sonde multi-éléments : résultats préliminaires," in *10ème Congrès Français d'Acoustique*, Lyon, 2010, pp. paper 286 – 6 pages.
- [5] C. Garnier, C. Lafon, and J.L. Dillenseger, "3-D Modeling of the Thermal Coagulation Necrosis Induced by an Interstitial Ultrasonic Transducer," *IEEE Transactions on Biomedical Engineering*, vol. 55, no. 2, pp. 833–837, 2008.